A new method to determine the elastoplastic properties of ductile materials by conical indentation

MA ZengSheng[1,2] ZHOU YiChun[1,2,*] LONG ShiGuo[1,2] & LU ChunSheng[3*]

[1]Key Laboratory of Low Dimensional Materials & Application Technology of Ministry of Education, Xiangtan University, Xiangtan 411105, China;

[2]Faculty of Materials, Optoelectronics and Physics, Xiangtan University, Xiangtan 411105, China;

[3]Department of Mechanical Engineering, Curtin University, Perth, WA 6845, Australia

Based on load-displacement curves, indentation is widely used to extract the elastoplastic properties of materials. It is generally believed that such a measure is non-unique and a full stress-strain curve cannot be obtained using plural sharp and deep spherical indenters. In this paper we show that by introducing an additional dimensionless function of $\Delta A / A$ (the ratio of residual area to the area of an indenter profile) in the reverse analysis, the elastoplastic properties of several unknown materials that exhibit visually indistinguishable load-displacement curves can be uniquely determined with a sharp indentation.

elastoplastic properties, indentation, reverse analysis

Hardness and elastic modulus measurements of a material by means of instrumented indentation have been a matter of discussion for many years. Generally, the elastoplastic properties of an engineering material are characterized by the elastic deformation, the onset of plastic deformation, and the subsequent strain hardening behavior [1–4]. Based on extensive finite element simulations and dimensional analysis, several scaling functions have been obtained in nanoindentation using sharp indenters, which can be used to determine material properties [5–7]. In describing the plastic deformation of metals, a power-law function is a somewhat good approximation and its corresponding stress-strain relationship under uniaxial tension can be represented as

$$\varepsilon = \begin{cases} \dfrac{\sigma}{E}, & \text{for } \sigma \le \sigma_y \\[2mm] \dfrac{\sigma_y}{E}\left(\dfrac{\sigma}{\sigma_y}\right)^{\frac{1}{n}}, & \text{others} \end{cases} \tag{1}$$

It is seen that there are three independent parameters, including the elastic modulus E, the initial yield strength σ_y, and the strain (or work) hardening exponent n. In the case of $n = 0$, eq. (1) is reduced to a model for elastic-perfectly plastic solids. For most metals and alloys, the values of Poisson's ratio v range between 0.25 and 0.35 and in this paper, $v = 0.3$ is assumed. To simulate the elastoplastic properties of metals, the elastic modulus E is chosen from 30 to 300 GPa, the yield strength of σ_y being from 30 to 3000 MPa, and the strain hardening exponent n being from 0 to 0.5.

In recent years, obtaining the three parameters (E, σ_y, n) in eq. (1) by indentation has been a focus of research [8]. Although a number of methods have been developed, it is still unclear whether these material properties could be

*Corresponding author (ZHOU YiChun, email: zhouyc@xtu.edu.cn; LU ChunSheng, email: C.Lu@curtin.edu.au)

1

uniquely determined by a load-displacement ($P-h$) curve. In the $P-h$ curve obtained from a bulk material, there are also three commonly used independent shape parameters: the loading curvature $C = P/h^2$, the contact stiffness $S = \mathrm{d}P/\mathrm{d}h\big|_{h=h_\mathrm{m}}^{\mathrm{unloading}}$, and the ratio $h_\mathrm{r}/h_\mathrm{m}$ between the residual penetration h_r and the maximum indentation depth h_m [6,9–11]. Based on dimensional analysis, the following dimensionless quantities have been proposed to characterize the shape of a $P-h$ curve [8,12]

$$\frac{P}{Eh^2} = \Pi_1\left(\frac{\sigma_\mathrm{y}}{E}, n\right) = \frac{C}{E}, \tag{2a}$$

$$\frac{S}{Eh^2} = \Pi_2\left(\frac{\sigma_\mathrm{y}}{E}, n\right) = \frac{bC}{E}\left(1 - \frac{h_\mathrm{r}}{h}\right)^{-1}, \tag{2b}$$

$$\frac{h_\mathrm{r}}{h} = \Pi_3\left(\frac{\sigma_\mathrm{y}}{E}, n\right), \tag{2c}$$

$$\frac{W_\mathrm{p}}{W_\mathrm{t}} = \Pi_4\left(\frac{\sigma_\mathrm{y}}{E}, n\right) = 1 - \frac{3}{1+b}\left(1 - \frac{h_\mathrm{r}}{h}\right), \tag{2d}$$

where W_p and W_t are the plastic work and the total work, respectively, and b is the exponent of a power-law fitting to the unloading curve, $P = C'\left(h - h_\mathrm{r}\right)^b$ with $C' = Ch_\mathrm{m}^2/\left(h_\mathrm{m} - h_\mathrm{r}\right)^b$ [12]. According to finite element simulations, b is independent of $W_\mathrm{p}/W_\mathrm{t}$. Therefore, of the four shape factors in eq. (2), only two are independent. That is, it is impossible to extract the mechanical properties (E, σ_y, n) by using a sharp indentation. Numerical studies have also shown that for a special group of materials (with different E, σ_y, and n), their $P-h$ curves are visually indistinguishable [12]. In order to obtain additional information, a dual (or plural) indenter was applied in indentation. Because of a lack of unique materials, Chen et al. [13,14] found out several unknown materials that cannot be distinguished by current techniques. Recently, we carried out the mathematical analysis on the non-unique problem of a reverse algorithm for measuring elastic-plastic properties by a sharp indentation [15]. We believe that there is still not a method that can be used to uniquely extract these mechanical properties (E, σ_y, n) from a sharp indentation.

To solve this problem, it is necessary to have an additional dimensionless function. Note that in indentation experiments, materials around the contact area tend to deform upwards (pile-up) or downwards (sink-in) with respect to the indented surface. A good understanding of the deformation zone around an indenter is of considerable importance because its shape determines the actual contact area between the indenter and specimen. In the case of sink-in, the contact area reduces and the pile-up in the contact area increases. These differences in surface deformation modes can affect the quantitative analysis of mechanical properties. Based on a high resolution electron back-scatter diffraction technique and finite element simulations, Wang et al. [16] showed the dependence of indentation pile-up patterns and microtextures on the crystallographic orientation of high purity copper single crystals. Wang et al. suggested that the pile-up patterns depend strongly on the crystallographic orientation of an indented surface. Patterns on the surfaces of (0 0 1), (0 1 1) and (1 1 1) oriented copper single crystals have four-, two-, and six-fold symmetry, respectively [16]. Zaafarani et al. found that the mobile dislocations are arranged around the indenter in a pattern similar to the pile-up distribution [17]. In fact, the peak values for the mobile dislocation density are in almost the same positions as the maximum pile-ups. As indentation proceeds, the peak of the mobile dislocation density migrates towards the sides of

the indenter. As a consequence of the dislocation activity, material flows along a path that has the least resistance. This tendency minimizes the strain energy and, since the contact area to the indenter acts as a rigid boundary, the most adequate path for the excess material is to flow towards the free surface, which leads to pile-ups. These patterns can be explained in terms of the pronounced out-of-plane displacement along the intersection vectors between the primary crystallographic slip and indented surface planes.

In consideration of the relationship between local plastic deformation and displacement patterns, a new dimensionless function, $\Delta A / A$, can be introduced, which is independent of the $P-h$ curve. As illustrated in Figure 1, ΔA is defined as an additional residual area related to the pile-up or sink-in after unloading, and A is the area of an indenter profile (relative to the original material surface) at h_{m}. Here, it is the material flow due to dislocation nucleation and glide that leads to the formation of pile-ups or mounds around the indentation site [18]. In the case of pile-up, the ΔA value is positive, and in sink-in it is negative.
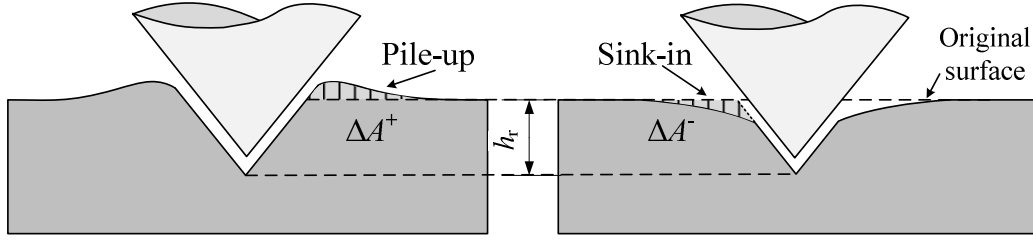

Figure 1   Schematic of pile-up and sink-in phenomena after unloading using a sharp indentation.

Combining with the anterior two independent dimensionless functions, we have

$$\frac{P}{Eh^2} = \Psi_1\left(\frac{\sigma_\mathrm{y}}{E}, n\right), \tag{3a}$$

$$\frac{W_\mathrm{p}}{W_\mathrm{t}} = \Psi_2\left(\frac{\sigma_\mathrm{y}}{E}, n\right), \tag{3b}$$

$$\frac{\Delta A}{A} = \Psi_3\left(\frac{\sigma_\mathrm{y}}{E}, n\right). \tag{3c}$$

Using an indenter with the half-apex angle $\theta = 70.3°$ as an example, finite element simulations were carried out by ABAQUS. As shown in Figure 2(a), Ψ_1 increases with the increase of the hardening exponent n and ratio σ_y/E. Conversely, Ψ_2 decreases with the increase of n and σ_y/E (see Figure 2(b)). Ψ_3 is approximately zero, corresponding to pile-up or sink-in profiles after unloading, as shown in Figure 2(c). By fitting simulation results, we obtain

$$\frac{P}{Eh^2} = \Psi_1\left(\frac{\sigma_\mathrm{y}}{E}, n\right) = \frac{-0.0389 + 0.6816n + 114.51(\frac{\sigma_\mathrm{y}}{E}) + 131.73(\frac{\sigma_\mathrm{y}}{E})^2}{1 - 0.5184n + 55.51(\frac{\sigma_\mathrm{y}}{E})}, \tag{4a}$$

$$\frac{W_\mathrm{p}}{W_\mathrm{t}} = \Psi_2\left(\frac{\sigma_\mathrm{y}}{E}, n\right) = 1.1843 - 0.3647n - 2.1725\left(\frac{\sigma_\mathrm{y}}{E}\right)^{0.4032}, \tag{4b}$$

$$\frac{\Delta A}{A} = \Psi_3\left(\frac{\sigma_y}{E}, n\right) = \frac{0.2195 - 0.3608n - 12.1331(\frac{\sigma_y}{E}) + 275.75(\frac{\sigma_y}{E})^2}{1 + 0.9078n + 17.922(\frac{\sigma_y}{E})}. \qquad (4c)$$
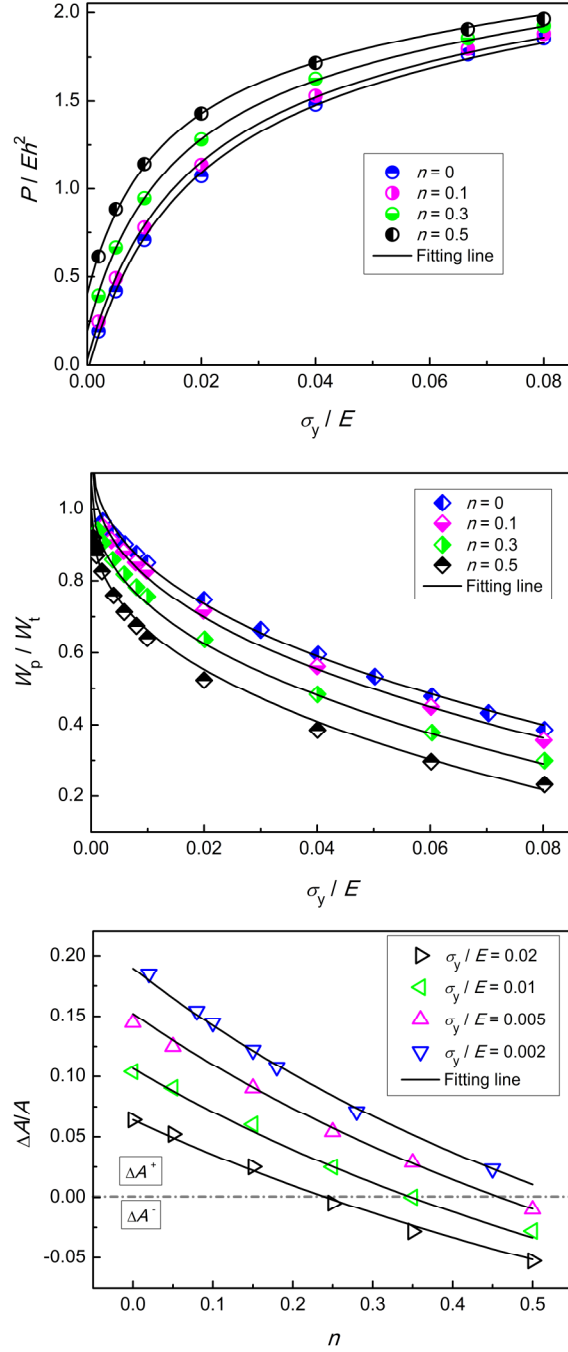

Figure 2 (Color online) Relationships between dimensionless functions and mechanical properties (σ_y/E and n) for (a) F/Eh^2, (b) W_p/W_t and (c) $\triangle A/A$. Symbols are numerical results from finite element simulations, and dash lines represent the fitting functions by using eq. (4). The data of W_p/W_t are from Cheng and Cheng [19].

Based upon these three dimensionless functions, Ψ_1, Ψ_2 and Ψ_3, the material properties can be determined by inverse analysis. For example, the elastoplastic properties (E, σ_y, n) of three different materials were estimated as (200 GPa, 2.36 GPa, 0), (200 GPa, 2.00 GPa, 0.1), and (200 GPa, 1.24 GPa, 0.3) [19], respectively (see Figure 3(a)). As shown in Figure 3(b), their indentation behaviors are indistinguishable from the loading and unloading curves. Therefore, it can be seen that with only a sharp indenter, the elastoplastic properties cannot be uniquely determined by eq. (2) from the $P-h$ curves. However, the A value can be obtained from the indentation profile at the maximum depth, which corresponds to ~0.349 μm^2. As shown in Figure 3(c), there is a significant difference of their pile-up effects after unloading, where ΔA are equal to 0.033, 0.025 and 0.014 μm^2, respectively. With the improved method or eq. (4), the elastoplastic properties (E, σ_y, n) of these three materials were determined as (194.18 GPa, 2.245 GPa, 0.0043), (214.84 GPa, 1.76 GPa, 0.133), and (242.32 GPa, 1.07 GPa, 0.323), which are consistent with the input data (see Figure 3(a)). It is obvious that such an improved method only requires one indentation test with a sharp indenter. It should be noted that, however, the expressions of dimensionless functions in eq. (4) are different for various indenters and friction coefficients between the indenter and material [20–22].
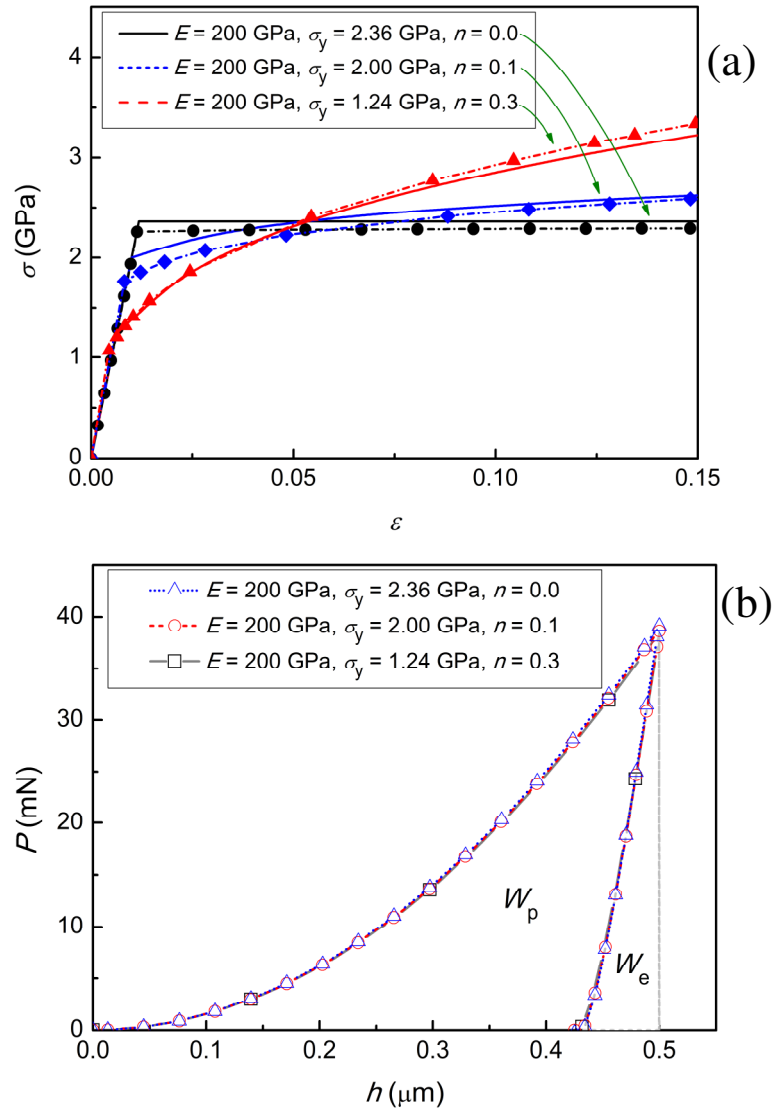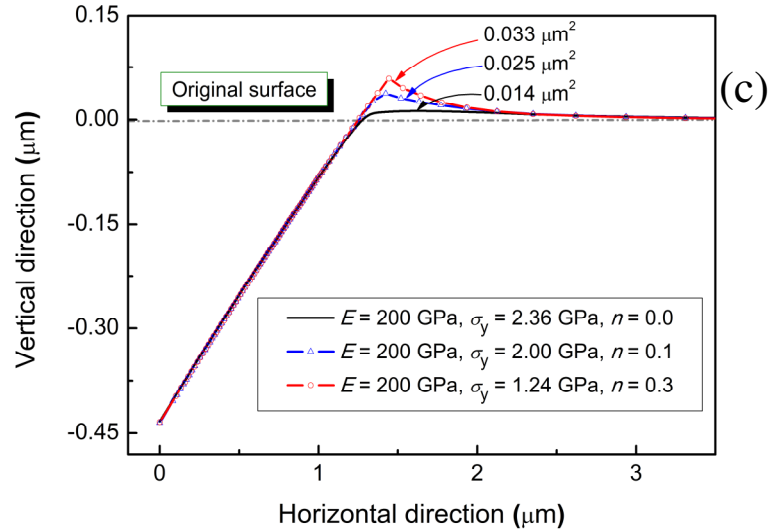
Figure 3 (Color online) Mechanical behaviors of three materials: (a) stress−strain curves (symbols represent results from the reverse analysis), (b) *P−h* curves (where W_e is the elastic work), and (c) indentation profiles after unloading.

In summary, by introducing another dimensionless function of $\Delta A / A$ in the reverse analysis, the elastoplastic properties of various materials can be distinguished. Based on a case study of indentation by an indenter with the half-apex angle $\theta = 70.3°$, it is shown that the improved method is efficient in characterizing a group of materials with visually indistinguishable load-displacement curves. It provides a useful guideline to properly use the indentation technique to measure the elastoplastic properties of ductile materials.

1   Tabor D. Indentation hardness: Fifty years on a personal view. Philos Mag A, 1996, 74: 1207–1212

2   Doerner M F, Nix W D. A method for interpreting the data from depth-sensing indentation instruments. J Mater Res, 1986, 1: 601–609

3   Oliver W C, Pharr G M. Improved technique for determining hardness and elastic modulus using load and displacement sensing indentation experiments. J Mater Res, 1992, 7: 1564–1583

4   Cheng Y, Cheng C. Relationships between hardness, elastic modulus, and the work of indentation. Appl Phys Lett, 1998, 73: 614–616

5   Myers S, Knapp J, Follstaedt D, et al. Mechanical properties of nickel ion-implanted with titanium and carbon and their relation to microstructure. J Appl Phys, 1998, 83: 1256–1264

6   Dao M, Chollacoop N, Van Vliet K J, et al. Computational modeling of the forward and reverse problems in instrumented sharp indentation. Acta Mater, 2001, 49: 3899–3918

7   Ogasawara N, Chiba N, Chen X. Representative strain of indentation analysis. J Mater Res, 2005, 20: 2225–2234

8   Cheng Y, Cheng C. Scaling, dimensional analysis, and indentation measurements. Mater Sci Eng R, 2004, 44: 91–149

9   Giannakopoulos A E, Suresh S. Determination of elastoplastic properties by instrumented sharp indentation. Scripta Mater, 1999, 40: 1191–1198

10   Zeng K, Chiu C H. An analysis of load-penetration curves from instrumented indentation. Acta Mater, 2001, 49: 3539–3551

11   Casals O, Alcalá J. The duality in mechanical property extractions from Vickers and Berkovich instrumented indentation experiments. Acta Mater, 2005, 53: 3545–3561

12   Alkorta J, Martinez-Esnaola J M, Sevillano J G. Absence of one-to-one correspondence between elastoplastic properties and sharp-indentation load-penetration data. J Mater Res, 2005, 20: 432–437

13   Chen X, Ogasawara N, Zhao M, et al. On the uniqueness of measuring elastoplastic properties from indentation: The indistinguishable mystical materials. J Mech Phys Solids, 2007, 55: 1618–1660

14   Liu L, Ogasawara N, Chiba N, et al. Can indentation technique measure unique elastoplastic properties? J Mater Res, 2009, 24: 784–800

15   Huang Y, Liu X, Zhou Y C, et al. Mathematical analysis on the uniqueness of reverse algorithm for measuring elastic-plastic properties by sharp indentation. J Mater Sci Technol, 2011, 27: 577–584

16   Wang Y, Raabe D, Kluber C, et al. Orientation dependence of nanoindentation pile-up patterns and of nanoindentation microtextures in copper single crystals. Acta Mater, 2004, 52: 2229–2238

17   Zaafarani N, Raabe D, Kluber C, et al. On the origin of deformation-induced rotation patterns below nanoindents. Acta Mater, 2008, 56: 31–42

18   Mordehai D, Kazakevich M, Srolovitz D J, et al. Nanoindentation size effect in single-crystal nanoparticles and thin films: A comparative experimental and simulation study. Acta Mater, 2011, 59: 2309–2321

19   Cheng Y, Cheng C. Can stress-strain relationships be obtained from indentation curves using conical and pyramidal indenters? J Mater Res, 1999, 14: 3493–3496

20   Taljat B, Pharr G M. Development of pile-up during spherical indentation of elastic-plastic solids. Int J Solids Struct, 2004, 41: 3891–3904

21   Bolshakov A, Pharr G M. Influences of pileup on the measurement of mechanical properties by load and depth sensing indentation techniques. J Mater Res, 1998, 13: 1049–1058

22   McElhaney K W, Vlassak J J, Nix W D. Determination of indenter tip geometry and indentation contact area for depth-sensing indentation experiments. J Mater Res, 1998, 13: 1300–1306